

Spectroscopic Observations of Thirteen Optically-selected QSOs in a Large Field Centred Around NGC 5334*

J. Surdej^{1,★}, J. P. Swings¹, H. C. Arp², and R. Barbier³

¹ Institut d'Astrophysique, Université de Liège, avenue de Cointe 5, B-4200 Cointe-Ougrée, Belgium

² Mount Wilson and Las Campanas Observatories of the Carnegie Institution of Washington, Santa Barbara Street 813, CA 9110, Pasadena, USA

³ European Southern Observatory, La Silla, Chile

Received May 18, accepted May 25, 1982

Summary. In order to further investigate the space density, distribution, and luminosity of quasars near as well as far from bright galaxies, a large field ($\sim 25 \text{ deg}^2$) around NGC 5334 was searched for QSO candidates with ultraviolet-excess.

A first step in this long term program consists here in a report on spectroscopic (IDS) data obtained with the ESO 3.6 m telescope for 13 quasars identified within a sample of 23 observed candidates. As normally expected, the redshift of these optically selected quasars falls in the range $Z_e \in [0.23, 2.08]$ with only one possible exception. Two, and possibly three, of the quasars of largest redshift show absorption lines.

The remaining 10 faint blue objects display zero-redshift stellar spectra.

Key words: quasars – redshift – spectroscopy – ultraviolet – excess objects

1. Introduction

With the aim of giving further evidence for or against the location of quasars in superclusters (see Oort, 1981; Oort et al., 1981) and/or nearby bright galaxies and their companions (cf. latest reviews by Arp (1980, 1981), we have recently initiated a long term program for collecting new observing material on the background density, distribution and luminosity of quasars in fields near bright galaxies as well as far from them (Arp and Surdej, 1982).

A first large field ($\sim 25 \text{ deg}^2$) centred around the Shapley-Ames galaxy NGC 5334 (Type: SB; mag: $B=11.9$) has been selected: adjacent ultraviolet and blue images were compared on a 48-inch Palomar Schmidt plate in order to search for QSO candidates. Twenty-three of these, randomly chosen, were observed spectroscopically at the European Southern Observatory and we report here about the spectra (redshift, equivalent width, line width, etc.) of thirteen quasars identified in this sample.

As soon as photometric data for the faint ultraviolet-excess objects become available, we intend to determine the limiting B magnitude and $U-B$ threshold of our survey as well as to derive, on

the basis of an additional dual exposure (U/B) Schmidt plate, a statistical value for the background density of quasars in the field of NGC 5334.

2. Observations

On 26 February 1979, a dual U/B exposure Schmidt plate (PS 25827) of a field centred around the spiral galaxy NGC 5334 [R.A. (1950) = $13^{\text{h}}50^{\text{m}}20^{\text{s}}$, Decl. (1950) = $-0^{\circ}52'06''$] has been taken with the 48-inch (1.2 m) Palomar Schmidt telescope. The ultraviolet exposure was 60 min behind a UG 1 filter and the blue exposure, offset 12" from the former one on the same baked 103 a-O emulsion, was 7 min, behind a GG 13 filter.

By visual inspection of the double image of a single object, quasar-candidates were chosen on the basis of their $U-B$ color index. In this selection, we roughly expect the ultraviolet threshold to be $U-B \sim -0.4$ and the limiting magnitude $B \sim 20.0$ mag. However, we plan to improve and re-derive the exact value of these photometric parameters in the near future.

On 1–3 April 1981, we have obtained spectra for twenty-three of these quasar-candidates using the IDS (Image Dissector Scanner) attached behind a Boller and Chivens spectrograph at the $f/8$ Cassegrain focus of the ESO 3.6 m telescope. The useful range of the IDS was 20 mm, giving an available spectral range from 3700 to 6700 Å approximately, with a characteristic drop in sensitivity below about 4000 Å. Using a $2'' \times 2''$ slit, we could achieve a resolution (FWHM) of 9 Å at a reciprocal dispersion near 171 Å/mm. Reduction of these spectra was performed with the "image handling and processing" system of ESO, at Garching by München.

For each faint blue object spectroscopically observed, a coordinate designation (resp. label $A-J$) for the identified quasars (resp. stars), 1950 coordinates and exposure times are listed in Table 1. The redshift measured for each quasar is also indicated in that Table. The equatorial coordinates, accurate to within $0''.3$, have been derived using the ESO Optronics measuring machine and the POS-programme package set up by West at the European Southern Observatory. Finding charts of all QSO candidates in the field around NGC 5334 will be published in a subsequent paper.

3. Spectroscopy of the 13 Identified Quasars

Table 2 lists for each quasar, ordered according to decreasing redshift, the observed emission line wavelengths corrected for the Earth's heliocentric motion ($V_{\odot} = 30 \text{ km s}^{-1}$) and a galactic

Send offprint requests to: J. Surdej

* Based on data collected at the European Southern Observatory, La Silla, Chile

** Chercheur Qualifié au Fonds National de la Recherche Scientifique (Belgium)

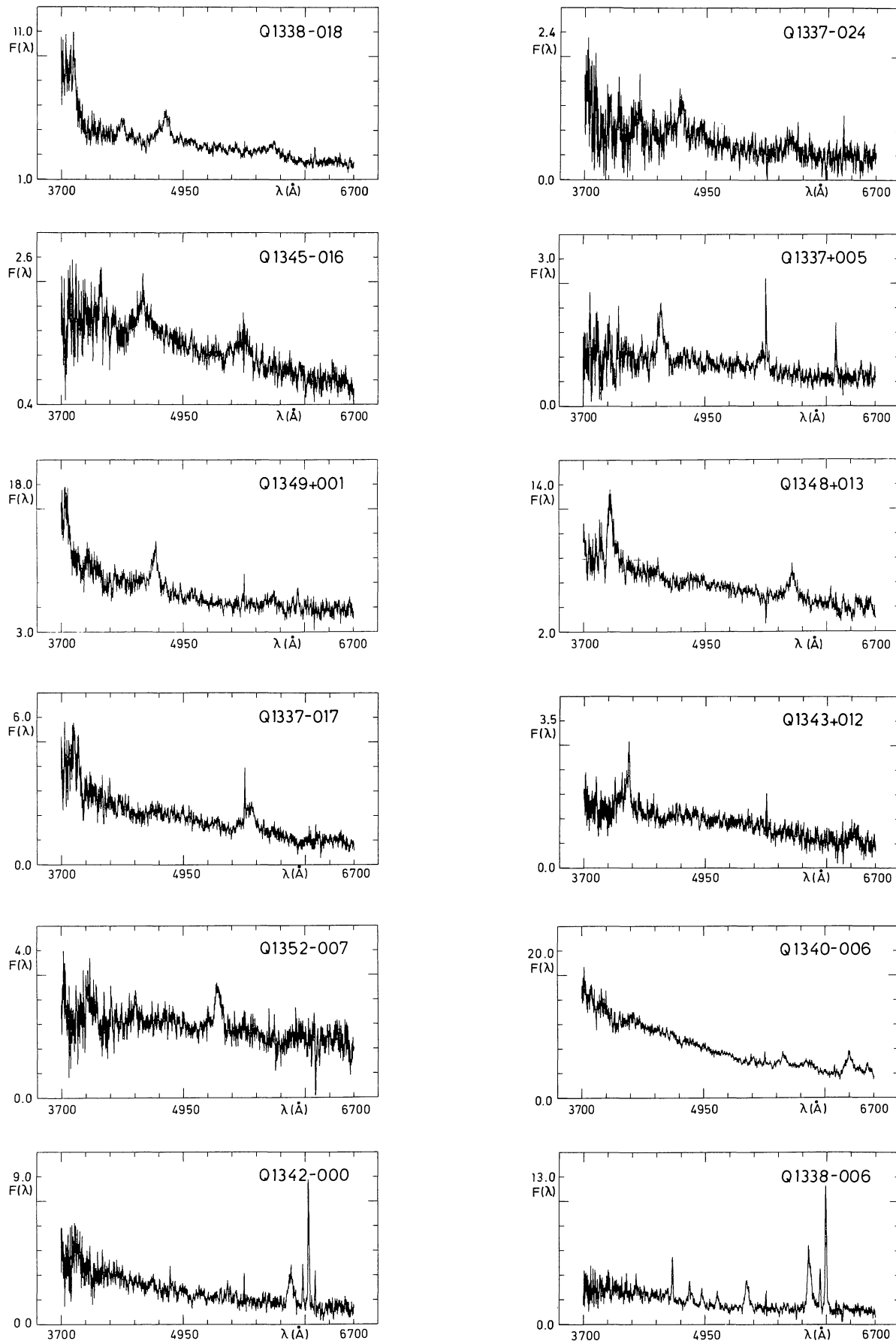


Fig. 1

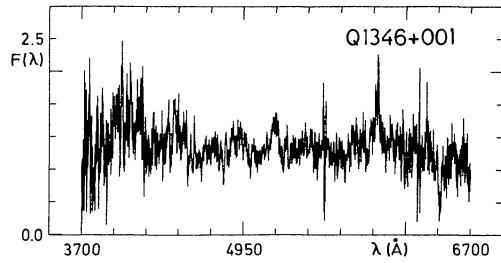


Fig. 1. Spectra of the 13 QSOs listed in Table 1. The abscissae correspond to the observed wavelengths in Å. The ordinate refers to a relative flux scale (see text)

Table 1. Observational data for the 23 spectroscopically observed quasar candidates

Object	R.A. (1950.0)	Decl. (1950.0)	Exposure time (min)	Redshift
1337−017	13 ^h 37 ^m 17 ^s 05 ± 0 ^s 02	−1°46′07″3 ± 0″3	20	1.010
1337−024	13 37 53.87	−2 24 09.7	30	2.035
1337+005	13 37 57.86	+0 30 17.6	30	1.902
1338−006	13 38 39.82	−0 38 06.9	10	0.237
1338−018	13 38 46.59	−1 53 48.8	20	2.079
1340−006	13 40 17.46	−0 38 39.6	20	0.326
1342−000	13 42 25.64	−0 00 58.6	10	0.245
A	13 42 35.40	−0 42 30.4	10	
B	13 42 41.78	+0 23 37.7	50	
C	13 43 11.48	+0 08 17.8	10	
1343+012	13 43 41.75	+1 12 04.6	50	0.487:
D	13 43 46.00	−0 39 10.7	10	
E	13 45 00.74	−0 37 30.7	10	
1345−016	13 45 14.56	−1 37 28.4	40	1.925
1346+001	13 46 44.05	+0 07 50.4	40	3.268:::
F	13 47 12.65	−2 33 27.3	20	
1348+013	13 48 55.23	+1 18 26.3	20	1.086
1349+001	13 49 16.75	+0 07 08.5	10	1.426::
G	13 51 21.59	−2 41 47.8	10	
H	13 52 19.37	−1 00 35.5	10	
1352−007	13 52 51.41	−0 43 00.7	20	0.422:
I	13 52 58.93	+0 26 04.2	10	
J	13 54 34.29	+1 19 31.3	10	

Note = : to ::: denotes increasing degree of uncertainty

Table 2a. Line identifications (Å) and associated redshifts

Quasar	Z_e	Si IV/O IV] 1401.62*	C IV 1549.48	He II 1640.4	C III] 1910.11 § or 1907.64	Remarks (Explanation below table)
1338−018	2.079 ± 0.002	4317.4 ± 1.4 ⁺ 1402.1	4768.4 ± 1.9 1548.6		5882.9 ± 0.1 : 1910.5	1
1337−024	2.035 ± 0.009	4249.8 ± 4.9 : 1400.3	4691.8 ± 1.1 1546.0		5815.3 ± 0.8 : 1916.2	2
1345−016	1.925 ± 0.008	4106.5 ± 0.2 : 1404.1	4537.0 ± 1.9 1551.3		5569.8 ± 0.3 1904.4	3
1337+005	1.902 ± 0.002	I.D.	4493.8 ± 0.1 1548.8	?	5544.7 ± 0.3 1911.0	4
1349+001	1.426 ± 0.012 ::		3747.4 ± 0.3 1544.4	3970.0 ± 1.3 1636.2	4655.6 ± 0.3 1918.7	5

Table 2b

Quasar	Z_e	C III] 1907.64 §	Mg II 2799.12	[O II] 3727.54	H γ + [O III]!	Remarks (Explanation below table)
1348+013	1.086 ± 0.002	3976.3 ± 0.5 1906.4	5842.0 ± 0.3 2800.9			
1337-017	1.010 ± 0.002	3831.3 ± 1.3 1906.5	5628.8 ± 0.3 2800.9			
1343+012	0.487 :		4160.8 ± 0.3 2799.1	?	6476.1 ± 2.8 4356.7	6
1352-007	0.422 ± 0.002 :		3977.7 ± 0.7 2796.6	5306.7 ± 0.2 3731.0	?	7

Table 2c

Quasar	Z_e	H γ + [O III]!	H β 4861.33	[O III] 4958.91	[O III] 5006.84	Remarks (Explanation below table)
1340-006	0.326 ± 0.001	5772.5 ± 0.1 4353.8	6448.1 ± 0.3 4863.4	I.D.	6635.5 ± 0.1 5004.7	8
1342-000	0.245 ± 0.001	?	6051.1 ± 0.4 4860.2	6174.3 ± 0.1 4959.1	6235.1 ± 0.1 5007.8	9
1338-006	0.237 ± 0.001	5378.0 ± 0.1 4346.1	6020.9 ± 0.1 4865.7	6132.5 ± 0.1 4955.9	6192.9 ± 0.1 5004.6	10
1346+001	3.268 ± 0.002 :::					11

Explanations of symbols

- * – See Wills and Netzer (1979) for the adopted rest wavelength of this blend
- § – See Wills (1980) and Ferland (1981) for the adopted rest wavelength of the C III] line transition when $Z_e > 1.8$ ($\lambda = 1910.11$ Å) and $Z_e < 1.8$ ($\lambda = 1907.64$ Å)
- + – The error estimates represent r.m.s. values as derived from three independent measurements of the line centers. Although we have, for most emission components, fitted the observed profile with a gaussian in order to derive the line center, these error estimates should be just considered as internal deviations of our measurements
- : – Somewhat uncertain value
- I.D. – Ill-defined but definitely present
- ? – Possibly present
- ! – Not taken into account in the determination of the redshift

Additional remarks to Table 2

- 1 At the extreme blue edge of the spectrum (see Fig. 1), Ly α + NV emission lines are present at $\lambda \sim 3740$ Å, but not measurable due to the too high noise background of the IDS data. One absorption line is clearly present in the blue wing of the C IV emission at $\lambda \sim 4564$ Å with an estimated equivalent width of about 3 Å.
- 2 C II λ 1334.53 is possibly present at $\lambda \sim 4054$ Å.

- 3 At least two absorption components, in the red wing of the Si IV emission line, at $\lambda \sim 4127$ and $\lambda \sim 4197$ Å, are present in the spectrum of this quasar. Better data are badly needed in order to study the absorption spectrum.
- 4 Absorption components at $\lambda \sim 4019$, 4236, and 4369 Å are suspected to be present in this QSO spectrum. It would be worthwhile to investigate this absorption spectrum on the basis of higher resolution and improved signal to noise data.
- 5 The uncertainty affecting this redshift determination is quite large and unsatisfactory. A redshift value $Z_e \sim 2.004$ cannot be totally excluded. Confirmation of either redshift value is mandatory. The presence of an emission-like feature at $\lambda \sim 5876$ Å remains doubtful.
- 6 The reported redshift is just based on one somewhat ill-defined line identified with Mg II. The presence of the H γ + [O III] blend at this same redshift renders our assumption quite plausible. Before being definitely accepted, this redshift value should be confirmed.
- 7 An emission-like feature at $\lambda \sim 4456$ Å remains unidentified. Confirmation of the proposed redshift value is needed.
- 8 There is some trace of Mg II λ 2799.12 at the extreme blue edge of the spectrum.
- 9 We suspect [O II] λ 3727.54 to be present at $\lambda \sim 4626.6 \pm 1.0$ Å.
- 10 The following emission lines [Ne V] λ 3425.8, [O II] λ 3727.54, [Ne III] λ 3868.74, and H δ , observed at $\lambda \lambda$ 4239.5 ± 0.1 , 4611.4 ± 0.1 , 4787.7 ± 0.1 , and 5075.5 ± 0.1 Å, respectively, were also included in the determination of the redshift value. The He

+ [Ne III] λ 3967.51 blend is well seen at λ 4916.2 \pm 0.3 Å and the He II λ 4685.68 and [Ne V] λ 3345.9 components are possibly present at λ \sim 5798 and λ \sim 4140 Å.

- 11 The exaggeratedly poor signal to noise ratio of this quasar spectrum prevents us from determining any trustworthy redshift value. The two broad emission lines observed at λ 5190.1 and 5981.0 Å are best identified with Ly α and Si IV/O IV]. If this is the case, Q 1346+001 would turn out to

be the highest redshift ($Z_e = 3.268 \pm 0.002$) quasar detected by the *U/B* technique. There are possible signs of the presence of the NV and C IV resonance doublets at λ \sim 5276, 6564 Å. Let us remark that redshift values such as $Z_e = 0.195, 2.147$, etc. cannot be totally excluded on the basis of the available data. Absorption components (see for instance at λ \sim 6460 Å) are also suspected to be present in this peculiar QSO spectrum. Better data are badly needed.

Table 3a. Full line width (km s⁻¹) and equivalent width (Å) of the emission components in the quasar rest frame

Quasar	Z_e	Si IV/O IV] 1401.62 *	C IV 1549.48	He II 1640.4	C III] 1910.11 § or 1907.64	Remarks (Explanation below table)
1338-018	2.079	2834 \pm 162 + 7.2 \pm 0.3	4594 \pm 260 18.4 \pm 0.3		2079 \pm 84: 4.6 \pm 1.2:	
1337-024	2.035	4852 \pm 270: 26.9 \pm 4.0:	3173 \pm 235 16.9 \pm 0.4		2715 \pm 58: 19.2 \pm 3.4:	
1345-016	1.925	1545 \pm 87: 4.6 \pm 0.3:	5249 \pm 259 14.4 \pm 0.7		3512 \pm 18 11.1 \pm 1.0	
1337+005	1.902	—	3641 \pm 146 25.5 \pm 0.8	?	3139 \pm 40.0 19.4 \pm 0.9	
1349+001	1.426 ::		> 4202 \pm 84 > 22.1 \pm 0.3	**	4505 \pm 212 14.7 \pm 0.2	1

Table 3b

Quasar	Z_e	C III] 1907.64 §	Mg II 2799.12	[O II] 3727.54	H γ + [O III]	Remarks (Explanation below table)
1348+013	1.086	4586 \pm 113 17.0 \pm 0.9	4705 \pm 134 16.4 \pm 0.6			
1337-017	1.010	**	7086 \pm 531 43.1 \pm 4.1			2
1343+012	0.487:		5310 \pm 219 46.9 \pm 1.4	?	5979 \pm 247 93.4 \pm 3.7	
1352-007	0.422:		**	7371 \pm 466 59.3 \pm 2.7	?	3

Table 3c

Quasar	Z_e	H γ + [O III]	H β 4861.33	[O III] 4958.91	[O III] 5006.84	Remarks (Explanation below table)
1340-006	0.326	6727 \pm 140 21.0 \pm 0.7	> 6227 \pm 142 > 67.8 \pm 1.3	I.D.	> 3562 \pm 83 > 23.7 \pm 1.4	4
1342-000	0.245	?	5108 \pm 127 77.3 \pm 2.5	1449 \pm 52 22.4 \pm 1.7	2113 \pm 53 91.7 \pm 1.1	5
1338-006	0.237	5363 \pm 239 61.7 \pm 2.7	4871 \pm 170 111.5 \pm 6.9	1495 \pm 46 30.8 \pm 2.1	3122 \pm 180 147.6 \pm 8.5	6
1346+001	3.268 :::					7

Explanations of symbols

- * – See Wills and Netzer (1979) for the adopted rest wavelength of this blend
- § – See Wills (1980) and Ferland (1981) for the adopted rest wavelength of the C III] line transition when $Z_e \geq 1.8$ ($\lambda = 1910.11 \text{ \AA}$) and $Z_e < 1.8$ ($\lambda = 1907.64 \text{ \AA}$)
- + – The error estimates represent r.m.s. values as derived from three independent measurements. Because the full line width and equivalent width of an emission line depend on the accurate setting of the continuum level, etc. one should be aware that the values reported in Table 3 are somewhat subjective and that the error estimates should just be considered as internal deviations of our measurements
- : – Somewhat uncertain value
- I.D. – Ill-defined
- ** – Very noisy data
- ? – Possibly present

Additional remarks to Table 3

- 1 Only lower limit values for the full width and equivalent width of C IV are given since the line is truncated on its blue wing (see Fig. 1).
- 2 No measurement is reported for C III] since the line is possibly truncated on its blue wing and located in a very noisy part of the spectrum.
- 3 The profile of the emission line at $\lambda \sim 5307 \text{ \AA}$, identified with [O II] $\lambda 3727.54$, is very asymmetrical.
- 4 As the red wing (resp. blue wing) of the H β (resp. [O III] $\lambda 5007$) line is superimposed on the [O III] $\lambda 4959$ emission component, the line width and equivalent width of the former ones have been systematically underestimated.
- 5 The full line width and equivalent width of [O II] $\lambda 3727.54$ are respectively $6456 \pm 184 \text{ km s}^{-1}$ and $15.1 \pm 0.8 \text{ \AA}$, in the rest frame of the quasar (see Table 2).
- 6 The full line width and equivalent width of the additional emission lines [O II] $\lambda 3727.54$, [Ne III] $\lambda 3868.74$, He I + [Ne III] $\lambda 3967.51$, and H δ are respectively found to be 2636 ± 334 , 20.2 ± 0.3 ; 6453 ± 530 , 31.9 ± 1.3 ; 4131 ± 377 , 23.1 ± 1.8 , and $4191 \pm 285 \text{ km s}^{-1}$, $24.1 \pm 1.1 \text{ \AA}$ in the rest frame of the quasar. When compared to the width of the Balmer emission lines, the forbidden lines display a relatively narrow emission peak. It is very likely that for the [O III] $\lambda 5006.84$ (and also possibly for the [Ne III] $\lambda 3868.74$) line transition(s), the narrow peak is superimposed on a much wider but fainter emission component (see Fig. 1).
- 7 Since the redshift of Q 1346 + 001 is very uncertain, the full line width and equivalent width of the lines observed at $\lambda \lambda 5190$ and 5981 \AA are hereafter expressed in the observer's rest frame. The measurements give: 6398 ± 200 , 31.6 ± 3.7 , and $6177 \pm 202 \text{ km s}^{-1}$, $40.8 \pm 3.6 \text{ \AA}$, respectively.

rotation of 250 km s^{-1} at the Sun. Wavelengths based on the redshift are also listed (second line) in the rest frame of the object. The mean error reported for each redshift in Table 2 is derived on the basis of an equal weight assigned to all emission lines definitely present in the QSO spectrum. Vertical bars give the wavelength limits of the observed part of the spectrum in the QSO rest frame. Whenever relevant, additional remarks appear at the end of that Table as well as an explanation of the symbols used therein. In

Table 3, we have similarly reported the full line width and equivalent width of all emission components in the rest frame of each quasar. For convenience, Tables 2 and 3 have been split in three sections corresponding to three sets of redshift: $Z_e > 1.4$; $1.4 > Z_e > 0.4$, and $Z_e < 0.4$.

Figure 1 illustrates the observed spectra from which the QSOs were confirmed and their redshift measured. Although standard photometric procedures were employed to reduce the observations to incident flux above the Earth's atmosphere (see Baldwin, 1975), the small aperture ($2'' \times 2''$) used and the poor weather conditions (clouds as well as variable seeing) prevailing on April 1–3 1981 definitely preclude from obtaining absolute spectrophotometry for the observed quasars. Therefore, in Fig. 1, the ordinates simply refer to a relative flux scale.

4. Discussion

With one possible exception, all redshifts reported in Table 2 fall in the range $Z_e \in [0.23, 2.08]$. It is well known (see Hewitt and Burbidge, 1980) that for redshifts $Z_e \geq 2.3$ the strong Ly α emission is shifted into the *B* passband – rendering unefficient the search of quasars by the present *U/B* technique: the observed distribution of redshifts (see Table 2) is thus about that normally expected.

Similarly, since it is well established that narrow absorption line systems mainly occur in the spectra of high-redshift QSOs (see Weymann et al., 1981) it is not surprising that absorption components have been detected in two (Q 1338 – 018 and Q 1345 – 016), and possibly three (Q 1337 + 005), of the four highest-redshift quasars identified in this survey.

The full line width and equivalent width measurements reported in Table 3 for each emission line in the QSO spectra will certainly contribute to enhance the set of observational data which continuously leads to the improvement of physical models for the line emitting regions surrounding the quasar nuclei. Referring to various works on the subject (Baldwin, 1977; Davidson and Netzer, 1979; Ferland, 1981; etc.) we may state that the observational data derived for the thirteen quasars in Table 3 lie well within the scatter affecting the mean composite spectrum of presently known quasars.

Acknowledgements. Part of this research has been supported by NATO grant No. 111/81. It is a pleasure to thank the night-assistants and/or operators Srs. Vega, Veliz, and Yagnam for their cheerful help at the telescope.

References

- Arp, H.: 1980, *Ann. NY Acad. Sci.* **336**, 94
- Arp, H.: 1981, *Astrophys. J.* **250**, 31
- Arp, H., Surdej, J.: 1982, *Astron. Astrophys.* (in press) (ESO preprint No. 164)
- Baldwin, J.A.: 1975, *Astrophys. J.* **201**, 26
- Baldwin, J.A.: 1977, *Monthly Notices Roy. Astron. Soc.* **178**, 67p
- Davidson, K., Netzer, H.: 1979, *Rev. Modern Phys.* **51**, 715
- Ferland, G.J.: 1981 (preprint)
- Hewitt, A., Burbidge, G.R.: 1980, *Astrophys. J. Suppl.* **43**, 57
- Oort, J.H.: 1981, *Astron. Astrophys.* **94**, 359
- Oort, J.H., Arp, H., de Ruiter, H.: 1981, *Astron. Astrophys.* **95**, 7
- Weymann, R.J., Carswell, R.F., Smith, M.G.: 1981, *Ann. Rev. Astron. Astrophys.* **19**, 41
- Wills, D., Netzer, H.: 1979, *Astrophys. J.* **233**, 1
- Wills, D.: 1980, *Astrophys. J.* **240**, 721